Superhigh-Throughput Needleless Electrospinning Using a Rotary Cone as Spinneret

Article *in* Small · August 2010

DOI: 10.1002/smll.201000454 · Source: PubMed

11 authors, including:

Bingan Lu
Hunan University
105 PUBLICATIONS **3,669** CITATIONS

SEE PROFILE

Jin Yuan Zhou
Lanzhou University
109 PUBLICATIONS **1,959** CITATIONS

SEE PROFILE

Zhenxing Zhang
Lanzhou University
127 PUBLICATIONS **2,722** CITATIONS

SEE PROFILE

Electrospinning

Superhigh-Throughput Needleless Electrospinning Using a Rotary Cone as Spinneret**

*Bingan Lu, Yajiang Wang, Yanxia Liu, Huigao Duan, Jinyuan Zhou, Zhenxing Zhang, Youqing Wang, Xiaodong Li, Wei Wang, Wei Lan, and Erqing Xie**

Nanomaterials have been playing increasingly important roles in industrial manufacturing due to their fascinating properties.[1–7] A number of synthesis methods, such as vapor–solid (VS),[8] vapor–liquid–solid (VLS),[9,10] solution–solid,[11] electrospinning, and solvothermal routes,[12] have been demonstrated for generating various nanostructures (nanowires, nanobelts, and nanotubes). Among those methods, electrospinning is one of the most intensively investigated approaches in the past two decades.[13–17] A typical electrospinning setup is comprised of a high-voltage power supply, a metal collector, and a glass syringe with a single metal needle.[18,19] In a typical electrospinning process, a polymer solution or melt is injected into the glass syringe and a liquid droplet forms at the tip of the metal needle. After applying a high voltage, the electrostatic charge will build up on the surface of the liquid droplet with an electric field as high as several kV cm^{-1}. When the quantity of charge reaches a certain value, under which a Taylor cone is formed, a continuous ultrathin fiber will be jetted from the bottom of the needle. The spun fibers are often collected on the surface of a metal collector. As well known, this electrospinning technique cannot be applied in industrial production due to its limited throughput (about 0.1 g h^{-1}).[20] Many efforts have thus concentrated on enhancing the productivity of the electrospinning technique. Ding et al.[21] and Theron et al.[22] have successfully spun fibers by using a multiple-jet electrospinning system. Although the output has been obviously enhanced by this approach, there still remain many challenges during those electrospinning processes, such as how to avoid interactions between each jet and how to clean the jets when they do not work. Dosunmu et al.[20] have developed an electrospinning technique equipped with a porous tube. With this method, the output has increased up to 5 g h^{-1}, which is 250 times more than that of traditional electrospinning. However, the preparation process of this method is instable, the collection of the nanofibers is not convenient, and the clogging problem of the porous tube is also difficult to solve. In view of the above points, Yarin et al.[23] have successfully electrospun nanofibers by using coactions of a normal magnetic and an electric field on a two-layer system, which consists of a lower ferromagnetic-suspension layer and an upper polymer-solution layer. The most outstanding advantage of this method is to solve a number of problems of multijet and /or porous systems. However, its electrospinning rate is only 12 times higher than that of traditional method. Nozzle-free centrifugal spinning of polymer nanofibers developed by Weitz et al.[24] offers an attractive alternative to electrospinning for the efficient, simple, and nozzle-free fabrication of fibers from a variety of polymer solutions. However, the diameter of the fibers fabricated in this way is not uniform, varying from 25 nm to 500 μm. Recently, Wang et al. obtained a high electrospinning rate by a novel electrospinning setup, which used a conical metal-wire coil as spinneret.[25] However, this needs a much higher voltage than traditional electrospinning. Therefore, it is still interesting to explore new electrospinning setups, which can satisfy the requirements of industrial production for commercial applications.

In this Communication, we report a needleless electrospinning setup using an electriferous rotating cone as the spinneret. The production throughput of this approach was about 10 g min^{-1}, which was several thousand times higher than that by traditional electrospinning technique with a single needle as the spinneret. The morphologies of the nanofibers fabricated by both traditional setup and this improved one were investigated by scanning electron microscopy (SEM). The principle of this new approach is also addressed in this paper. Additionally, the effects of electrospinning speed and the voltage between the cone and the collector (V_{CC}) of this electrospinning system on the properties of the fibers are discussed. The improvement of this method might open new doors to many potential industrial applications of electrospinning technique.

A schematic of this high-throughput electrospinning system is shown in Figure 1A. It consisted of four major components: a high-voltage power supply, a metallic cone, a direct-current

[*] Dr. B. Lu, Dr. Y. Wang, Dr. Y. Liu, Dr. H. Duan, Dr. J. Zhou Dr. Z. Zhang, Dr. Y. Wang, Dr. X. Li, Dr. W. Wang, Dr. W. Lan Prof. E. Xie
Key Laboratory for Magnetism and Magnetic Materials of the Ministry of Education
Lanzhou University
Lanzhou 730000, Gansu (P. R. China)
E-mail: xieeq@lzu.edu.cn

[**] This work was financially supported by the National Natural Science Foundation of China (No. 50802037), partially by the Natural Science Foundation of Gansu Province in China (Grant No: 0710RJZA041), and the Fundamental Research Funds for the Central Universities (No.lzujbky-2009-56).

Supporting Information is available on the WWW under http://www.small-journal.com or from the author.

DOI: 10.1002/smll.201000454

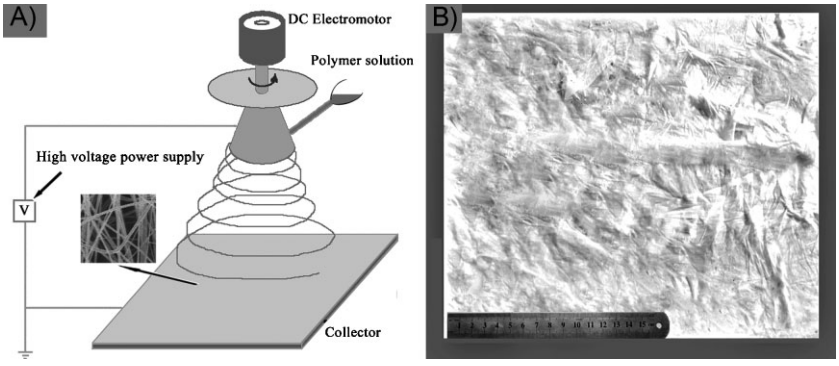

Figure 1. A) Schematic of the electrospinning setup that used a rotating cone as the spinneret (inset: a typical SEM image of the nonwoven mat of PVP nanofibers deposited on the collector). B) A photograph of an electrospun PVP-fiber membrane fabricated using the above setup.

(DC) electromotor, and a collector. When using an aluminum conveyor belt as the collector, the resultant electrospun nanofiber membrane was very long. Figure 1B presents the poly (vinyl pyrrolidone) (PVP)-fiber membrane prepared at $V_{CC} = 30\,kV$, with a cone-collector distance of 20 cm, electrospinning time of 15 min, and electrospinning throughput of $10\,g\,min^{-1}$. The PVP-fiber membrane was $30 \times 30\,cm^2$ and the maximal PVP-fiber membrane was up to $30 \times 60\,cm^2$. After spinning, the membrane with well dispersive nanofibers could be conveniently transferred to other substrates for further characterization and application. To obtain highly aligned electrospun nanofibers, two parallel aluminum plates were used as the collector in this novel cone-spinneret setup. Between the parallel plates, fibers can be aligned very well.[26,27] Figure 2A shows an SEM image of nanofibers prepared by a single-needle electrospinning system with an inner needle diameter of 0.5 mm, a needle–collector distance of 15 cm, V_{CC} of 18 kV, an electrospinning rate of $0.63\,g\,h^{-1}$, and an electrospinning time of 1 h. The diameter of the nanofibers was between 30–170 nm, mainly located at ≈100 nm. Figure 2B shows SEM images of the nanofibers prepared by the superhigh-throughput electrospinning system at a cone–collector distance of 20 cm, the V_{CC} of 36 kV, an electrospinning rate of $10\,g\,min^{-1}$, and an electrospinning time of 5 min. The fibers obtained had uniform diameters of between 220–320 nm, mainly located at ≈250 nm (Figure 2D). The morphologies of these nanofibers prepared by the novel cone-spinneret setup were nearly same as those by the traditional electrospinning technique with a single spinneret (Figure 2C and D) but the electrospinning rate was 950 times faster than that of the single-needle electrospinning system. It is believed that this electrospinning rate fully satisfies the requirements of industrial production and could be further improved by using a larger rotating metallic cone. By changing the distance between parallel aluminum plates, superhigh-throughput electrospinning aligned nanofiber arrays with lengths up to centimeters could be obtained.

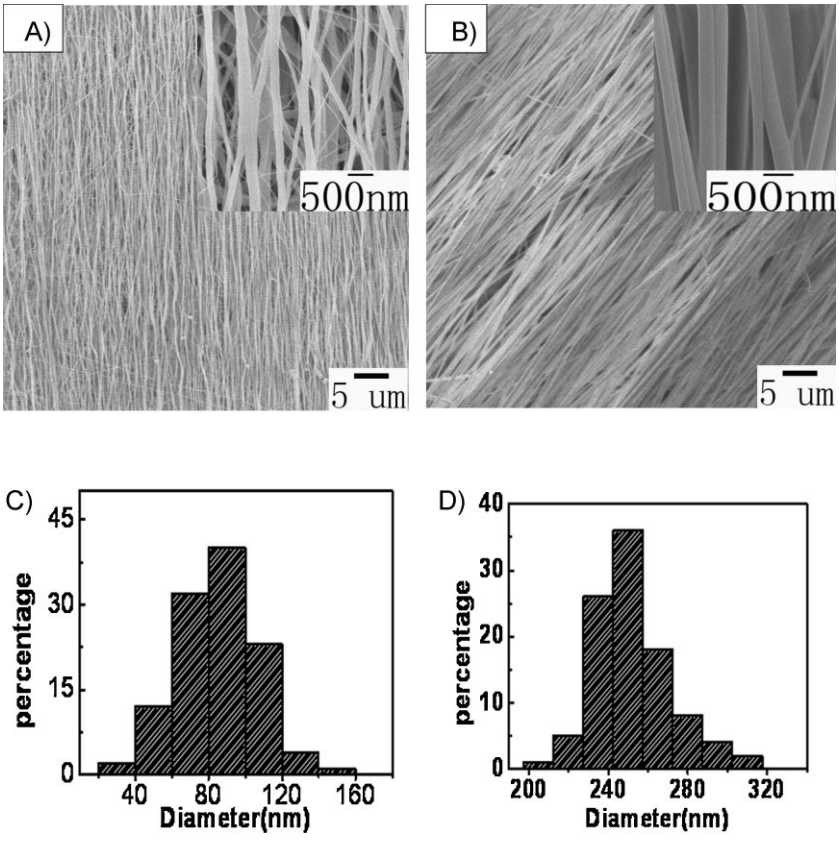

Figure 2. SEM images of highly aligned PVP nanofibers array prepared by A) 60-min single-needle electrospinning and B) 5 min of the superhigh-throughput electrospinning system. Histograms showing the size distribution of nanofibers prepared by C) single-needle electrospinning and D) superhigh-throughput electrospinning system (the size distribution was obtained from the SEM images of 100 nanofibers).

In order to study the electrospinning mechanism of our improved setup, a theoretical analysis is presented in Figure 3. Figure 3A shows a typical schematic of the electrospinning process. At the start of the electrospinning process, many mist-like fibers formed at the lower edge of the rotating cone. Subsequently, those formed fibers would be thrown off from the cone and new fibers would form at the edge. Finally, the nanofibers would be continuously fabricated and collected on the collector. Figures 3B–F shows a schematic illustration of the electrospinning process by using an electriferous rotating cone as the spinneret. When one drop of the PVP solution was transferred to the surface of the cone, it could be electrified with positive charges immediately. The charged liquid droplet would flow along the rotating surface under the coactions of gravity, the moment of inertia, and the electric force. Once the liquid droplet reached the lower

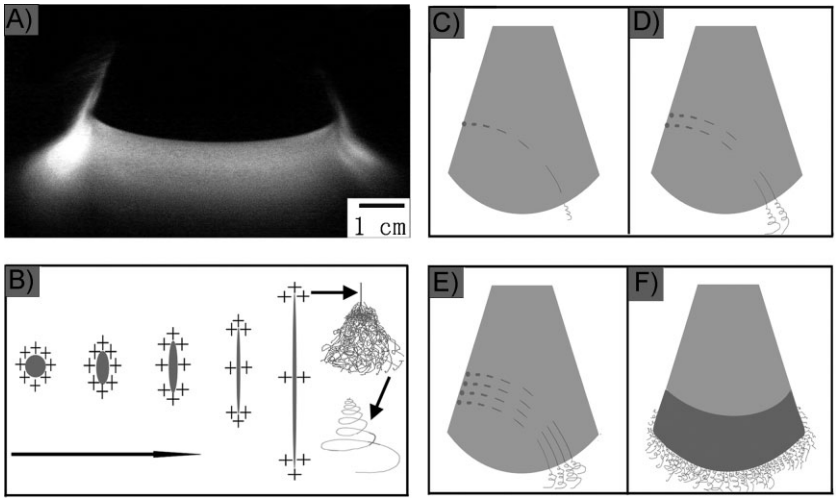

Figure 3. The scheme of electrospinning mechanism: A) Digital photograph illustration of the electrospinning process of PVP solution in the dark room; B) Flow chart of the formation of the fibers; C–F) Progress of substance movement and transformation on the cone surface as the solution drop flowed on the surface of the rotating cone.

edge of the cone, the electrospinning process started. In our earlier experiments, no fibers, but many droplets, were observed on the collector under high electric field ($1.5\,kV\,cm^{-1}$) for this improved setup when the metal cone was kept static or rotated slowly (<20 rpm). We found that a minimum rotating speed of 50 rpm was necessary for the formation of fibers and stable electrospinning. Actually, it was seen that a few microfibers or nanofibers could be even generated under the condition that the cone was rotating (100 rpm) and no voltage was applied in this electrospinning setup. Therefore, we believe that both rotation and electric field were the crucial factors in this electrospinning system. Thus, the formation mechanism of the needleless process can be illustrated as below (Figure 3B). First, under the mechanical action of the rotation movement, the charged liquid droplet was stretched and deformed from a round to a thin elliptical shape gradually; the liquid droplet could even be stretched into microfibers or nanofibers directly.[24] Then, when the bending angle of the elliptically shaped liquid droplet was close to that of the Taylor cone that formed in the traditional single-needle electrospinning process, the deformed liquid droplet would begin to spin nanofibers under the high electric field. With continuous feeding of the polymer solution, the number of spinnerets would increase quickly and thousands of similar spinnerets would eventually form around the lower circumferential edge of the rotating cone (Figure 3C–F). Thus, the production rate increased up to

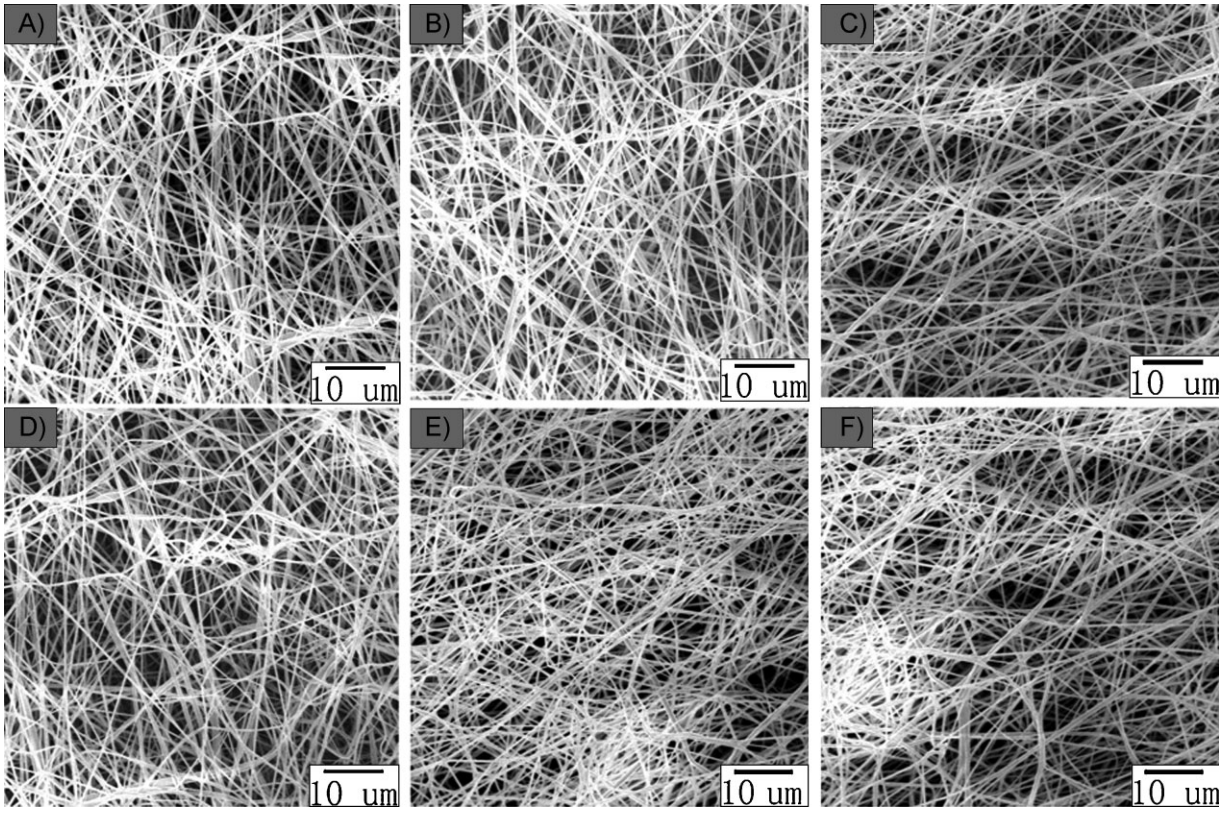

Figure 4. SEM images of electrospun PVP nanofibers at different electrospinning rates: A) 5.0, B) 7.7, C) 8.3, D) 9.1, E) 10.0, and F) 12.5 g min^{-1}, with a voltage between the cone and the collector of 30 kV and a distance between the cone and the collector of 20 cm.

thousands of times more than that of the traditional single-needle system accordingly.

Similarly to the situation with the single-needle electrospinning system, the diameter of PVP nanofibers might be varied by different electrospinning parameters. In traditional electrospinning, the diameters of nanofibers increase with increasing electrospinning throughput. However, by using this superhigh-throughput electrospinning technique, the diameter of the fibers did not obviously change in spite of the increased electrospinning throughput (Figure 4). When electrospinning throughput was 5.0 g min^{-1}, the diameter of the fibers varied from 180 to 500 nm with an average diameter of ≈320 nm (Figure 4A). When the electrospinning throughput increased to 7.7, 8.3, 9.1, and 10.0 g min^{-1}, the diameters of fibers were 220–510, 230–510, 250–510, and 260–510 nm with average diameters of approximately 330, 333, 336, and 340 nm (Figure 4B–E), respectively. Even when the throughput increased to 12.5 g min^{-1}, there was still no significant change in the diameter distribution (the diameters of fibers varied from 300 to 520 nm with an average diameter of ≈350 nm, as shown in Figure 4F). It can be seen from above results that increasing the flow rate of electrospinning did not significantly change the maximum diameter of the fibers, while the minimum diameter of the fibers increased and no significant change in the statistical average diameter was observed, so the average error of the diameter decreased (Figure 6A). This means that, in a certain range, the fibers became more uniform with increasing electrospinning rate. In industrial production, the liquid flow rate is usually difficult to accurately control. With this method, the flow rate has little effect on the diameter of the fibers, which provides convenience for industrial production.

The value of V_{CC} was another key factor determining the morphology and diameter of the electrospun fibers. If the V_{CC} was <6 kV (keeping the distance between the cone and the collector at 20 cm), the solution could not be fully stretched, leading to a number of beads in the fibers (Figure 5A). When V_{CC} was increased to 12 kV, the beads disappeared, resulting in fibers with diameters of 600–1000 nm (Figure 5B). With increasing V_{CC}, the diameters of the fibers further decreased and became more uniform. The diameters of the fibers decreased to 400–850 nm (Figure 5C), 300–650 nm (Figure 5D), 250–510 nm (Figure 4D), and 220–320 nm (Figure 2B) as V_{CC} increased to 18, 24, 30, and 36 kV, respectively, which means that V_{CC} played an important role in controlling the diameter of the electrospun fibers. With V_{CC} increasing in a certain range, the diameters of the fibers decreased and the average error of the diameter also decreased (Figure 6B). For industrial production, the voltage is relatively easy to control accurately and, with a rotating cone, the diameter of the fibers can be controlled by changing the value of V_{CC} in this superhigh-throughput electrospinning process, which also provides convenience for industrial production.

In summary, we demonstrated a new superhigh-throughput electrospinning technique with a large metal rotating cone as the spinneret. The typical production rate by this method is ≈10 g min^{-1}, which is 1000 times more than that of the traditional electrospinning method. Nanofibers could be obtained as highly aligned arrays with lengths up to several centimeters by modifying the collector. In addition, we found

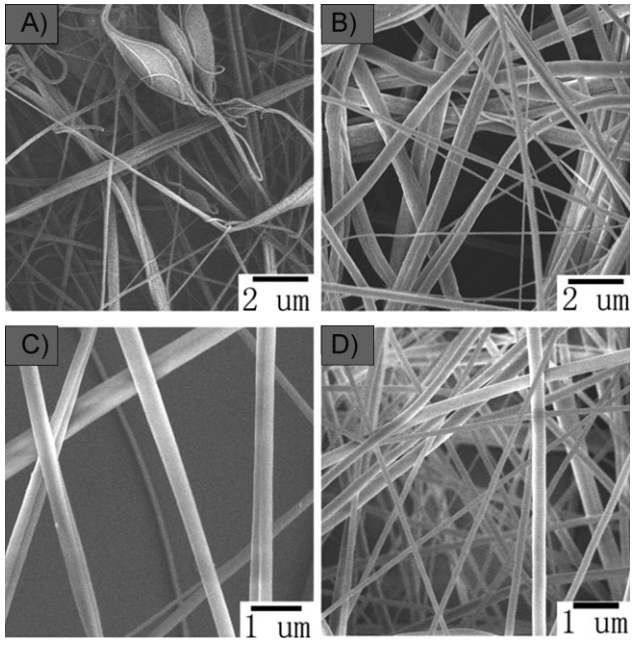

Figure 5. SEM images of PVP electrospun nanofibers at different electric fields: cone–collector voltages of A) 6, B) 12, C) 18, and D) 24 kV, with an electrospinning throughput of 8.3 g min^{-1} and a distance between the cone and the collector of 20 cm.

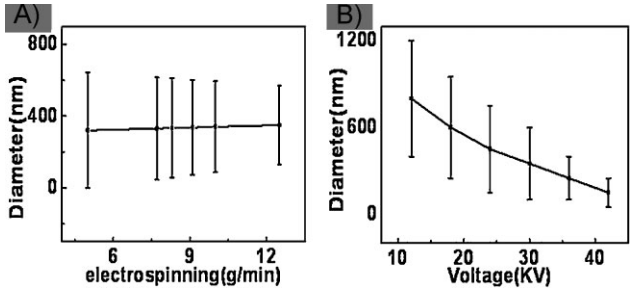

Figure 6. Average diameter of the fibers and average error of the diameter: A) Average diameter of the fibers and average error of the diameter at different electrospinning throughputs, with a voltage between the cone and the collector of 30 kV and a distance between the cone and the collector of 20 cm; B) Average diameter of the fibers and average error of the diameter at different voltages, with an electrospinning throughput of 8.3 g min^{-1} and a distance between the cone and the collector of 20 cm.

that it was the value of V_{CC} that affected the diameter of the electrospinning fibers, while the electrospinning rate had not-obvious effects on the diameter. This technique provides a method for the industrial production of nanofibers.

Experimental Section

The hollow metal rotary cone was used as spinneret (Figure 1A). The bottom and top diameters, the height, and the thickness of the hollow cone were 30, 7, 40, and 2 mm, respectively. The cone was fixed coaxially to the DC electromotor with a nylon column. At the top of the nylon column, there was a plastic wafer with a thickness of 0.5 mm and a diameter of 40 mm. The nylon

column and the plastic wafer were used to avoid static electricity. The outer surface of the cone was mechanically polished. Pieces of copper wires were brushed up against the cone as electrical contacts.

PVP (Sigma-Aldrich, $M_w \approx 1\,300\,000$) solution flowed onto the cone. PVP solution was prepared by dissolving the PVP powder in absolute ethyl alcohol (≥99.7%) and stirring for 0.5 h[28] (the mass ratio of PVP to absolute ethyl alcohol was 14:1). Next, the PVP solution was transferred to the surface of the rotating cone by a glass pipe with an inner diameter of ≈0.15 cm. During the electrospinning process, the rotational speed of the cone was typically kept at 100 rpm, the typical V_{CC} was 30 kV, the cone–collector distance was 20 cm, the typical electrospinning throughput was 10 g min^{-1}, and the typical preparation time was 10 min. The electrospun nanofibers were collected on a large aluminum sheet or aluminum foil parallel to the aluminum conveyer in air.[18,29] The diameter of the nanofibers were compared at different electrospinning throughputs (5.0, 7.7, 8.3, 9.1, 10.0, and 12.5 g min^{-1}, respectively, with the same V_{CC} of 30 kV) and V_{CC} (6, 12, 18, 24, 30, and 36 kV, respectively, with the same electrospinning throughput of 8.3 g min^{-1}), with a distance between the cone and the collector of 20 cm.

Keywords:
electrospinning · nanofibers · rotary cones · superhigh throughput

[1] Y. Cui, Q. Wei, H. Park, C. M. Lieber, *Science* **2001**, *293*, 1289.
[2] M. M. Stevens, J. H. George, *Science* **2005**, *310*, 1135.
[3] A. Tuteja, W. Choi, M. Ma, J. M. Mabry, S. A. Mazzella, G. C. Rutledge, G. H. McKinley, R. E. Cohen, *Science* **2007**, *318*, 1618.
[4] J. Yuan, X. Liu, O. Akbulut, J. Hu, L. S. Suib, J. Kong, F. Stellaccl, *Nat. Nanotechnol.* **2008**, *3*, 332.
[5] M. Bognitzki, W. Czado, T. Frese, A. Schaper, M. Hellwig, M. Steinhart, A. Greiner, J. H. Wendorff, *Adv. Mater.* **2001**, *13*, 70.
[6] N. A. Kotov, J. O. Winter, I. P. Clements, E. Jan, B. P. Timko, S. p. Campidelli, S. Pathak, A. Mazzatenta, C. M. Lieber, M. Prato, R. V. Bellamkonda, G. A. Silva, N. W. S. Ka, F. Patolsky, L. Ballerini, *Adv. Mater.* **2009**, *21*, 3970.
[7] H. Ko, Z. Zhang, Y. L. Chueh, J. C. Ho, J. Lee, R. S. Fearing, A. Javey, *Adv. Funct. Mater.* **2009**, *19*, 3098.
[8] C. Liu, Z. Hu, Q. Wu, X. Wang, Y. Chen, H. Sang, J. Zhu, S. Deng, N. Xu, *J. Am. Chem. Soc.* **2005**, *127*, 1318.
[9] Y. Wu, P. Yang, *J. Am. Chem. Soc.* **2001**, *123*, 3165.
[10] K. A. Dick, K. Deppert, T. Martensson, B. Mandl, L. Samuelson, W. Seifert, *Nano Lett.* **2005**, *5*, 761.
[11] Z.-P. Sun, L. Liu, L. Zhang, D. Z. Jia, *Nanotechnology* **2006**, *17*, 2266.
[12] C. Zhang, Z. Kang, E. Shen, E. Wang, L. Gao, F. Luo, C. Tian, C. Wang, Y. Lan, J. Li, X. Cao, *J. Phys. Chem. B* **2005**, *110*, 184.
[13] V. Kalra, J. H. Lee, J. H. Park, M. Marquez, Y. L. Joo, *Small* **2009**, *5*, 2323.
[14] Y. Dror, W. Salalha, R. Avrahami, E. Zussman, A. L. Yarin, R. Dersch, A. Greiner, J. H. Wendorff, *Small* **2007**, *3*, 1064.
[15] D. Li, J. T. McCann, Y. Xia, *Small* **2005**, *1*, 83.
[16] X. H. Li, C. L. Shao, Y. C. Liu, *Langmuir* **2007**, *23*, 10920.
[17] P. Katta, M. Alessandro, R. D. Ramsier, G. G. Chase, *Nano Lett.* **2004**, *4*, 2215.
[18] D. Li, Y. Xia, *Adv. Mater.* **2004**, *16*, 1151.
[19] X. Lu, C. Wang, Y. Wei, *Small* **2009**, *5*, 2349.
[20] O. O. Dosunmu, G. G. Chase, W. Kataphinan, D. H. Reneker, *Nanotechnology* **2006**, *11*, 1123.
[21] B. Ding, E. Kimura, T. Sato, S. Fujita, S. Shiratori, *Polymer* **2004**, *45*, 1895.
[22] S. A. Theron, A. L. Yarin, E. Zussman, E. Kroll, *Polymer* **2005**, *46*, 2889.
[23] A. L. Yarin, E. Zussman, *Polymer* **2004**, *45*, 2977.
[24] R. T. Weitz, L. Harnau, S. Rauschenbach, M. Burghard, K. Kern, *Nano Lett.* **2008**, *8*, 1187.
[25] X. Wang, H. Niu, T. Lin, X. Wang, *Polym. Eng. Sci.* **2009**, *49*, 1582.
[26] D. Li, Y. Wang, Y. Xia, *Adv. Mater.* **2004**, *16*, 361.
[27] M. Zhou, J. Zhou, R. Li, E. Q. Xie, *Nano. Res. Lett.* **2010**, *5*, 279.
[28] J. Zhou, M. Zhou, Z. Chen, Z. Zhang, C. Chen, R. Li, X. Gao, E. Q. Xie, *Surf. Coat. Technol.* **2009**, *203*, 3219.
[29] J. Zhou, Z. Chen, M. Zhou, X. Gao, E. Xie, *Nano. Res. Lett.* **2009**, *4*, 814.

Received: March 18, 2010
Revised: April 30, 2010
Published online: July 2, 2010